Marine Environmental Research 112 (2015) 9–20

Contents lists available at ScienceDirect

Marine Environmental Research

journal homepage: www.elsevier.com/locate/marenvrev

Phytoplankton biomass and composition in a well-flushed, sub-tropical estuary: The contrasting effects of hydrology, nutrient loads and allochthonous influences

J.A. Hart [a], E.J. Phlips [a, *], S. Badylak [a], N. Dix [b], K. Petrinec [b], A.L. Mathews [c], W. Green [d], A. Srifa [a]

[a] Fisheries and Aquatic Sciences Program, SFRC, University of Florida, 7922 NW 71st Street, Gainesville, FL 32653, USA
[b] Guana Tolomato Matanzas National Estuarine Research Reserve, 505 Guana River Road, Ponte Vedra, FL 32082, USA
[c] Georgia Southern University, Department of Biology, Statesboro, GA 30460, USA
[d] St. Johns River Water Management District, 4049 Reid Street, Palatka, FL 32177, USA

ARTICLE INFO

Article history:
Received 10 March 2015
Received in revised form
28 July 2015
Accepted 31 August 2015
Available online 4 September 2015

Keywords:
Guana Tolomato Matanzas estuary
Red tides
Karenia brevis
Water residence time
Eutrophication
Climate change

ABSTRACT

The primary objective of this study was to examine trends in phytoplankton biomass and species composition under varying nutrient load and hydrologic regimes in the Guana Tolomato Matanzas estuary (GTM), a well-flushed sub-tropical estuary located on the northeast coast of Florida. The GTM contains both regions of significant human influence and pristine areas with only modest development, providing a test case for comparing and contrasting phytoplankton community dynamics under varying degrees of nutrient load. Water temperature, salinity, Secchi disk depth, nutrient concentrations and chlorophyll concentrations were determined on a monthly basis from 2002 to 2012 at three representative sampling sites in the GTM. In addition, microscopic analyses of phytoplankton assemblages were carried out monthly for a five year period from 2005 through 2009 at all three sites. Results of this study indicate that phytoplankton biomass and composition in the GTM are strongly influenced by hydrologic factors, such as water residence times and tidal exchanges of coastal waters, which in turn are affected by shifts in climatic conditions, most prominently rainfall levels. These influences are exemplified by the observation that the region of the GTM with the longest water residence times but lowest nutrient loads exhibited the highest phytoplankton peaks of autochthonous origin. The incursion of a coastal bloom of the toxic dinoflagellate *Karenia brevis* into the GTM in 2007 demonstrates the potential importance of allochthonous influences on the ecosystem.

1. Introduction

Increased cultural eutrophication throughout the world has raised concerns about the future integrity of many coastal ecosystems (Nixon, 1995). Among the major components of aquatic ecosystems, phytoplankton are often the most directly and rapidly affected by nutrient enrichment, therefore, phytoplankton are widely used indicators of eutrophication and trophic status (Carlson, 1977; Cloern, 2001; Gupta, 2014). Anthropogenically-driven increases in nutrient loads have been linked to increased occurrences and intensities of algal blooms in many water bodies throughout the world (Hallegraeff, 2003; Glibert and Burkholder, 2006; Anderson et al., 2008; Heisler et al., 2008; O'Neil et al., 2012), however, predicting the responses of phytoplankton communities in coastal ecosystems to changes in nutrient load can be challenging due to the influences of mitigating physical, chemical and biological conditions (Mallin et al., 1999; Howarth et al., 2000; Cloern, 2001; Smayda, 2008; Paerl et al., 2014; Harding et al., 2015; Phlips et al., 2015). Classic 'single signal, single response' conceptual models, inspired by studies of eutrophication in lakes (Vollenweider, 1976), are often poor predictors of phytoplankton biomass in dynamic estuarine environments. For example, annual nutrient loads are higher in San Francisco Bay than in Chesapeake Bay, yet average primary production in San Francisco Bay is 20 times lower than in Chesapeake Bay (Cloern, 2001). In San Francisco Bay mitigating factors contribute to the resistance of

* Corresponding author.
E-mail addresses: Phlips@ufl.edu (E.J. Phlips), nikki.dix@dep.state.fl.us (N. Dix), alorenmathews@gmail.com (A.L. Mathews), wgreen@sjrwmd.com (W. Green).

http://dx.doi.org/10.1016/j.marenvres.2015.08.010
0141-1136/

phytoplankton production and biomass to increases in nutrient load, including short water residence times, top-down pressure from benthic grazer communities and shifts in the character of nutrient elements, particularly nitrogen (Alpine and Cloern, 1992; Cloern and Dufford, 2005; Glibert et al., 2014). Understanding the nature of such mitigating factors is of central importance in defining the responses of phytoplankton to differences in nutrient load (Cloern, 2001; Lucas et al., 2009).

The Guana Tolomato Matanzas (GTM) estuary is an example of a subtropical well-flushed ecosystem where regional differences in nutrient loads are not fully reflected in spatial patterns of phytoplankton biomass and composition (Phlips et al., 2004; Dix et al., 2013). Such flushed ecosystems are widespread throughout the world, but they have not been as extensively studied as those in temperate environments (Cloern et al., 2014). The GTM contains regions of significant human influence, such as the watersheds associated with St. Augustine, the oldest city in the United States (i.e. founded in 1565). Other regions of the GTM are characterized by relatively pristine watersheds with minimal human development. The GTM also contains regions of differing levels of tidal flushing. Regions near inlets to the Atlantic Ocean have water residence times on the order of days, while areas more distant from inlets have water residence times on the order of weeks (Sheng et al., 2008). The spatially diverse characteristics of the GTM provide an opportunity to examine the contrasting effects of nutrient load and water residence times on phytoplankton biomass and composition. In general, well-flushed estuaries, which experience relatively short water residence times, are often characterized by lower phytoplankton biomass and different community structure than more restricted ecosystems with similar nutrient loads (Knoppers et al., 1991; Monbet, 1992; Phlips et al., 2004; Badylak et al., 2007; Harrison et al., 2008; Lucas et al., 2009; Phlips et al., 2010). On the other hand, strong exchange of water with the coastal environment can also subject well-flushed ecosystems to incursions of coastal harmful algal blooms (HAB), including toxic red tide species (Steidinger, 1983; Heil et al., 2014).

In this study, the relationships between the phytoplankton community, hydrologic conditions (e.g. water residence times) and nutrient loads in the GTM were examined over a 10-year period, which included both drought and flood years, providing some insights into the effects of climatic variability. The GTM was incorporated into the National Estuarine Research Reserve System (NERRS) of the U.S. National Oceanographic and Atmospheric Administration (NOAA) in 1999, highlighting the importance of the ecosystem as a coastal marine resource, in part because of its location in the southeastern coast of North America and the diversity of habitat types within the system, including keystone oyster and salt marsh communities (Frazel, 2009). Over the past few decades some of the watersheds associated with the GTM have begun to experience significant human development, accentuating the need for water quality information that can assist in the design of management plans aimed at protecting this valuable aquatic resource. This paper examines one key aspect of this need for information, namely the sensitivity of phytoplankton communities within the GTM to temporal and spatial differences in nutrient load.

2. Methodology

2.1. Site description and sampling sites

The study area included the Guana River, Tolomato River and Matanzas River estuaries located on the northeast coast Florida, together designated as the GTM (Fig. 1). The Guana and Tolomato River estuaries lie north of the St. Augustine Inlet and the Matanzas estuary lies south of the St. Augustine Inlet in the vicinity of the Matanzas Inlet. The GTM is an inner shelf lagoon that forms part of the Intracoastal Waterway along the east coast of the United States. The GTM is characterized by a May through October warm wet season and November through April cool dry season. The GTM is also subject to tropical storm activity which can affect water quality conditions (Dix et al., 2008).

Water samples were collected at three NERRS System-wide Monitoring Program sites within the GTM from 2002 through 2012. The northern most sampling site was located at Pine Island in the Tolomato River, 16 km north of the St. Augustine Inlet, and designated PI (Fig. 1). Mean depth at PI was 3.1 m. Land use in the associated watershed includes 81% upland forests, wetlands, and surface waters; 13% urban/residential, and 5% agriculture/rangeland (FDEP, 2008). Water residence times in the Pine Island region are several fold longer than in the St. Augustine and Matanzas regions of the GTM. A hydrologic study in the spring of 2004 showed that water residence times (i.e. 50% water turnover time) in the Pine Island region averaged 15 days, compared to 2 days in the Matanzas region and 3 days in the St. Augustine region (Sheng et al., 2008).

The second sampling site was located near the outflow of the San Sebastian River, and designated SS (Fig. 1). The San Sebastian River receives drainage from the city of St. Augustine (FDEP, 2008). Mean depth at SS was 3.7 m. Land use in the associated watershed includes 68% upland forests, wetlands, and surface waters; 28% urban/residential, and 4% agriculture/rangeland (FDEP, 2008). Site SS is tidally influenced by the St. Augustine Inlet, which is located approximately 5 km north of the sampling site.

The third sampling site was located approximately 4 km north of the Matanzas Inlet and designated FM (Fig. 1). Mean depth at FM was 2.5 m. The region of the GTM where FM is located is characterized by relatively undeveloped watershed. Land use in the associated watershed includes 83% upland forests, wetlands, and surface waters; 15% urban, and 2% agriculture/rangeland (FDEP, 2008).

2.2. Field collections

YSI 6600 and YSI 6600 EDS multi-parameter data sondes were deployed at the three sampling sites at approximately mid-water column. Temperature and salinity were recorded at 30-min intervals from January 2002 to December 2006 and at 15-min intervals from January 2007 to December 2012. Water quality data, including total nitrogen (TN), total phosphorus (TP), silica (Si), colored dissolved organic matter (CDOM), Secchi disk depth (SD), and chlorophyll *a* (CHL), were downloaded from the NERRS Centralized Data Management Office website (http://www.nerrsdata.org/).

Water samples were collected monthly from 2003 through 2012 with an integrating sampling tube which captures water from the surface to within 0.1 m from the bottom. Water samples were used for subsequent analysis of colored dissolved organic matter (CDOM), total phosphorus (TP), total nitrogen (TN), silica (Si), chlorophyll *a* and phytoplankton composition. Samples withdrawn for water chemistry analysis were maintained on ice for return to the laboratory. Aliquots of water for chlorophyll *a* analysis were filtered onto 0.7 μm filters (i.e. Whatman GF/F) on site and stored frozen until analysis. Aliquots of water for CDOM analyses were filtered through 0.7 μm filters (i.e. Whatman GF/F) on site and stored on ice.

Water samples for phytoplankton analysis were collected from 2005 through 2009. Samples were preserved with Lugols solution. Aliquots of water for picophytoplankton analysis were kept frozen (i.e. −20 °C) until analysis within 48 h of collection using autofluorescence microscopy (Phlips et al., 1999).

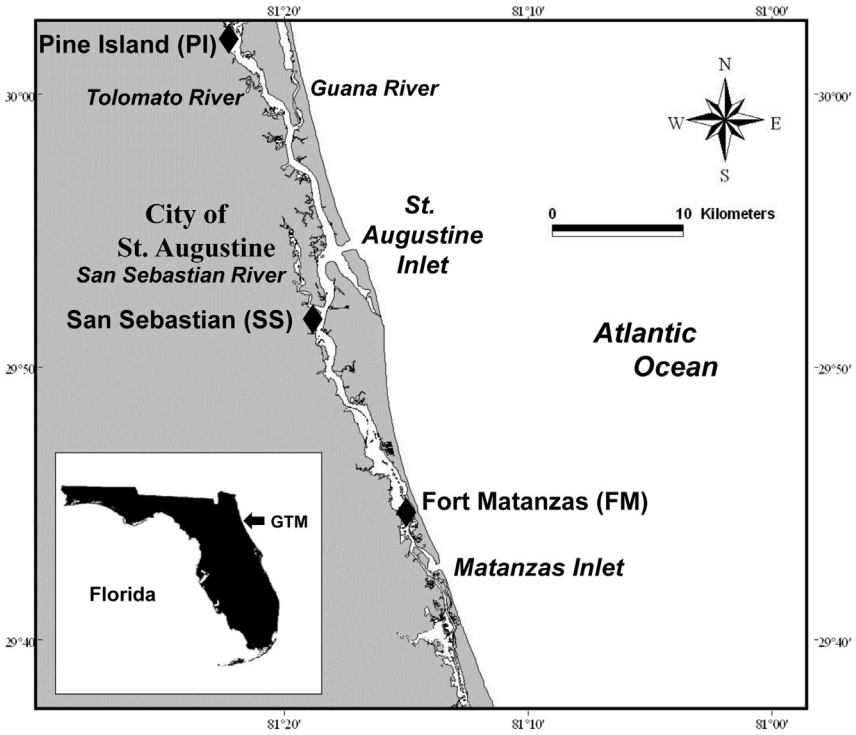

Fig. 1. Sampling site locations within the GTM; Pine Island (PI), St. Augustine (SS), Fort Matanzas (FM).

2.3. Chemical analyses

Total nitrogen (TN) was determined using the persulfate digestion method (APHA, 1998; Parsons et al., 1984) and analyzed with a Bran-Luebbe AutoAnalyzer. Total phosphorus (TP) was determined using the persulfate digestion method (APHA, 1998; Parsons et al., 1984) using a dual beam scanning spectrophotometer. Silica (Si) was determined by the ammonium molybdate method using a dual-beam scanning spectrophotometer (APHA, 1998). Inorganic nutrient concentrations, i.e. dissolved inorganic nitrogen ($NO_2 + NO_3 + NH_4^+$) and soluble reactive phosphorus (PO_4^+) were determined colorimetrically with a Bran-Luebbe AutoAnalyzer (Parsons et al., 1984; APHA 1998) using filtered aliquots of sample water (Gelman GF/F glass fiber filters).

Colored dissolved organic matter (CDOM) was determined using a dual-beam scanning spectrophotometer against a platinum–cobalt standard solution (APHA, 1998).

Chlorophyll *a* concentration was determined using a dual beam spectrophotometer after extraction of the filtered samples with 90% warm ethanol (Sartory and Grobbelaar, 1984).

All collection, preservation and analyses methods followed guidelines set forth by the NELAP QAQC Accreditation #E72883.

2.4. Rainfall data

Rainfall data was obtained from the U.S. Climatological Data site for the St. Augustine meteorological station in Florida (U.S. Climatological Data, www7.ncdc.noaa.gov/IPS).

2.5. Nutrient load estimates

External nutrient loads were calculated as the sum of modeled watershed loading, direct atmospheric deposition and point discharge from wastewater treatment plants that file monthly reports to the Florida Department of Environmental Regulation (FDEP). Modeling of watershed loads was performed using an adaptation of the Pollutant Load Screen Model (PLSM) (Adamus and Bergman, 1995), which was calibrated to loading data collected from watersheds in the GTMNERR (Green and Steward, 2003; Green, 2013). PLSM is a GIS–based model that simulates watershed loading using empirically derived mean discharge coefficients and nutrient concentrations based upon land cover, soil hydrologic group and annual Doppler rainfall. Treatment coefficients were applied to runoff loading from areas receiving Environmental Resource Permits for those years following issuance of such permits. For this investigation, the model was modified to predict total nitrogen and phosphorus loading from runoff and base flow on an annual time-step from 2002 through 2012. Loads were calculated for three segments of the GTM associated with each sampling site, 1) the Pine Island segment, starting 6 km north of the St. Augustine Inlet to 23 km north of the St. Augustine Inlet, 2) the San Sebastian segment, starting 2 km south of the St. Augustine Inlet to 11 km south of the St. Augustine Inlet, and 3) Fort Matanzas segment, starting from the Matanzas Inlet to 10 km north of the Matanzas Inlet. Comparison of model loads to those measured in studied catchments of the GTMNERR indicate PLSM-predicted N and P loads were within 6% and 14%, respectively, of measured loads in 2012 (Green, 2013).

2.6. Phytoplankton analysis

Microscopic analysis of phytoplankton composition was conducted using the Utermöhl method (Utermöhl, 1958). Preserved samples were settled in 19 mm inner diameter cylindrical chambers. Phytoplankton cells were identified and counted at 400X and 100X with a Nikon phase contrast inverted microscope. At 400X, a minimum of 100 cells of a single taxa and 30 grids was counted. If 100 cells were not counted within 30 grids, up to a maximum of 100 grids was counted until one hundred cells of a single taxa was reached. At 100X a total bottom count was completed for taxa

greater than 30 microns. Phytoplankton species were identified to the lowest practical unit using the aforementioned standard light microscopy techniques. Some taxa were designated at higher levels of classification and placed into size classes (e.g. centric diatoms) in lieu of routinely carrying out additional procedures beyond the practical scope of this project (e.g. clearing out cytoplasm from diatoms to examine detailed frustule structure for speciation).

Fluorescence microscopy was used to enumerate picoplanktonic cyanobacteria at 1000× magnification (Phlips et al., 1999). Subsamples of seawater were filtered onto 0.2 μm Nuclepore filters and mounted between a microscope slide and cover slip with immersion oil.

Cell biovolumes were estimated by assigning combinations of geometric shapes to fit the characteristics of individual taxa. Specific phytoplankton dimensions were measured for at least 30 randomly-selected cells. Volumes were calculated for each cell type (Smayda, 1978). Taxa exhibiting a range of cell sizes, such as occurs with many diatom species, were divided into size classes to provide more accurate estimates of biovolume. The total biovolume per sample was calculated as the sum of the estimated cell volumes for each species.

For the purpose of description and discussion, 'blooms' were defined as phytoplankton biovolumes for individual species which fell within the top 25% of biovolumes observed over the study period for all individual species; i.e. $> 1.2 \times 10^6$ μm^3 ml^{-1}.

Potentially toxic or problematic species were identified using the harmful algal bloom species lists (HAB species) of the Intergovernmental Oceanographic Commission of UNESCO (http://www.ioc-unesco.org/hab/) and Florida Fish and Wildlife Research Institute (http://www.research.myfwc.com).

2.7. Statistical analyses

Selected environmental parameters were z-scaled and used to perform Principle Component Analyses (PCAs) to determine multivariate relationships among parameters and sampling sites. Multi-dimensional principle component (PC) axes were suggested by within-group sum-square plots. Results are shown on the space of the first two PCs and accounted for 61% of explained variation.

3. Results

3.1. Physical–chemical parameters

Rainfall – Monthly rainfall totals were generally greater during the wet (May–October) than dry season (Fig. 2). Total annual rainfall was highest in 2005 (178 cm), a strong tropical storm year, and lowest in 2010 (92 cm). Other annual rainfall totals (from lowest to highest) included, 95 cm (2006), 105 cm (2011), 109 cm (2008), 127 cm (2004), 135 cm (2002), 136 cm (2003), 143 cm (2012), 147 cm (2007) and 150 cm (2009).

Water temperature – Mean monthly water temperatures generally ranged from 15 °C to 30 °C, reflecting the sub-tropical location of the GTM (Fig. 3). The lowest mean monthly winter water temperature were observed in 2003/04, 2010/11 and 2011/12, i.e. near 12 °C. The lowest individual winter temperature minima was 5 °C at PI in December 2010. Mean monthly summer water temperatures were often several degrees higher at PI than SS or FM, reflecting the higher rates of tidal water exchange with the Atlantic Ocean at SS and FM.

Salinity – Mean monthly salinities at SS and FM generally ranged from 30 to 36 psu, reflecting the strong tidal water exchanges at these two sites (Fig. 4). The greatest range in mean monthly salinity was observed at Site PI (i.e. 13 to 38 psu), where tidal water exchange is less than at SS or FM, and water residence

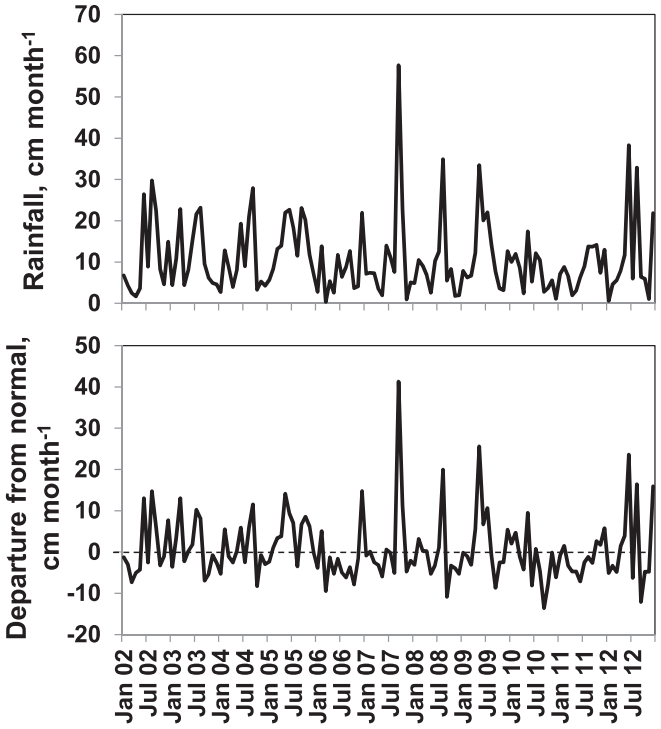

Fig. 2. Monthly rainfall totals and departures from normal at the St. Augustine meteorological station (U.S. Climatological Data, www7.ncdc.noaa.gov/IPS).

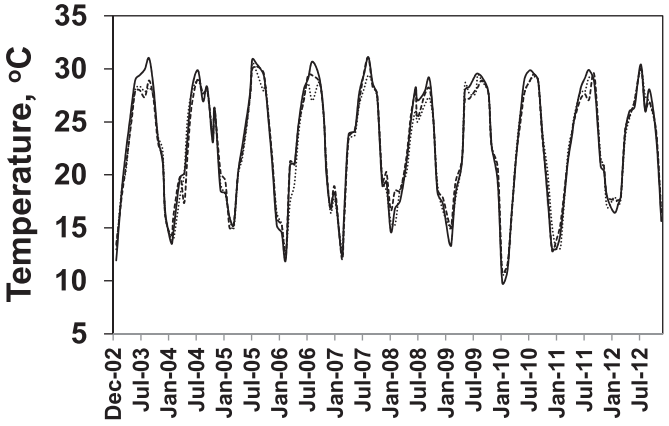

Fig. 3. Water temperatures at the three sampling sites; PI (solid line), SS (dotted line) and FM (dashed line).

times are several fold longer (Sheng et al., 2008). Dips in salinity were observed at all three sites during periods of high rainfall, most prominently at PI (Fig. 4). Salinity ranges during the relatively high rainfall years of 2002–2005, 2009 and 2012 were lower than during the relatively dry years of 2006–2008 and 2010–2011 at all three sites (Fig. 4).

Secchi depth – Mean Secchi disk depths (SD) were from 1.0 to 1.4 m at all three sites (Table 1). Mean wet season SD values were slightly shallower than during the dry season.

Colored dissolved organic matter – Mean wet and dry season colored dissolved organic matter (CDOM) levels were similar at FM and SS, ranging from 14 to 18 pcu (Table 1). Mean CDOM values were higher at PI than SS or FM, most notably during the wet season (57 pcu), reflecting the influence of inflows from the watershed.

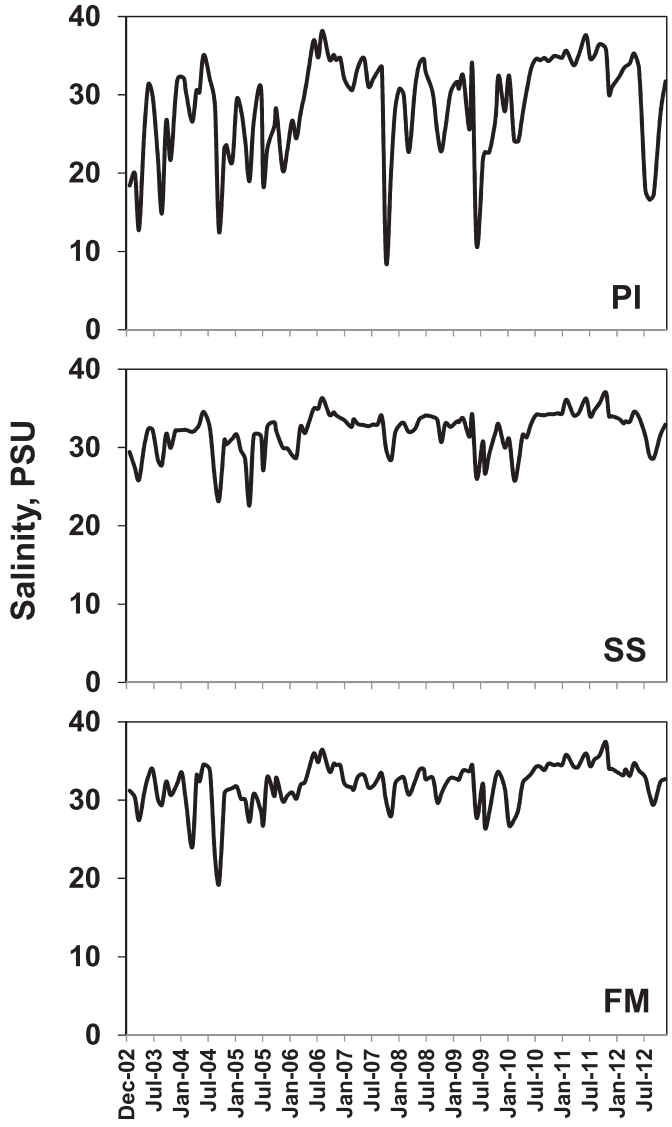

Fig. 4. Salinity at the three sampling sites; PI (top panel), SS (middle panel) and FM (bottom panel).

Nutrient concentrations and loads – Mean total phosphorus (TP), soluble reactive phosphorus (SRP), total nitrogen (TN), dissolved inorganic nitrogen (DIN) and silica (Si) concentrations were lower during the dry season than wet season at all three sites (Table 1). Mean nutrient concentrations were generally higher at PI than at FM or SS, and higher at SS than FM, for each season (Table 1).

Table 2
Annual total nitrogen (TN) (kg ha^{-1} yr^{-1}) and total phosphorus (kg ha^{-1} yr^{-1}) load per estuarine region, i.e. Pine Island (PI), St. Augustine (SS) and Fort Matanzas (FM).

Year	PI	SS	FM	PI	SS	FM
	TN	TN	TN	TP	TP	TP
2003	6	79	28	0.5	12.3	2.9
2004	15	108	78	1.3	16.9	8.1
2005	32	147	72	2.7	23.2	7.4
2006	9	39	24	0.8	6.6	2.8
2007	17	70	53	1.5	11.6	5.7
2008	26	79	62	2.2	12.0	6.8
2009	48	125	128	4.1	19.4	14.0
2010	9	25	18	0.8	4.3	2.3
2011	7	40	9	0.6	6.6	1.1
2012	36	70	35	3.0	11.6	3.8

Annual external nitrogen and phosphorus loads were higher in the San Sebastian segment of the GTM than either Pine Island or Fort Matanzas segments (Table 2). TP loads in the St. Augustine region were 2–4 times higher than in the Matanzas region, and 4 to 10 times higher than in the Pine Island region. Similarly, TN loads in the San Sebastian segment were 1.5–4 times higher than in the Fort Matanzas segment and 2 to 10 times higher than in the Pine Island segment. The high mean TP and TN concentrations at PI relative to SS and FM are attributable to the higher water exchange rates with the Atlantic Ocean at the latter two sites.

Chlorophyll – Mean chlorophyll *a* (CHL) concentrations were lower during the dry season than wet season at all three sites (Table 1). The latter trend can also been seen in the CHL time series for the three sites (Fig. 5).

Mean CHL concentrations were highest at PI and lowest at FM in both the wet and dry seasons (Table 1). The spatial trend is observable in the CHL time series for the three sites (Fig. 5). Wet season peaks in CHL concentration were often in excess of 10 μg L^{-1}, at PI but only rarely higher than 10 μg L^{-1} at SS and FM, with the major exception being 2007, when an off-shore dinoflagellate bloom entered the estuary.

Relationships between water column parameters – The results of PCA analysis demonstrate basic relationships between selected water column parameters in the GTM for 2002–2012 (Fig. 6A). Chlorophyll *a* was correlated to temperature, reflecting the seasonal pattern of phytoplankton biomass. Total nitrogen, total phosphorus and silica concentrations were negatively correlated to salinity, but positively related to CDOM, showing the influence of freshwater runoff from the watershed on nutrient concentrations. Secchi disk depths were negatively correlated to chlorophyll *a* and CDOM, reflecting the influence of the two parameters on light transmission through the water column.

Table 1
Mean values for selected water column parameters in the dry (November–April) and wet (May–October) seasons. Parameters include total phosphorus (TP, μg L^{-1}), soluble reactive phosphorus (SRP, μg L^{-1}), total nitrogen (TN, μg L^{-1}), dissolved inorganic nitrogen (DIN, μg L^{-1}), silica (Si, mg L^{-1}), chlorophyll *a* (CHL, μg L^{-1}), colored dissolved organic matter (CDOM, platinum cobalt units), and Secchi disk depth (SD, m^{-1}). Standard deviations are shown in parentheses.

	PI		SS		FM	
	Dry	Wet	Dry	Wet	Dry	Wet
TP	59 (20)	76 (25)	54 (21)	63 (23)	45 (13)	56 (18)
SRP	16 (9)	26 (15)	12 (7)	20 (12)	11 (6)	17 (8)
TN	469 (182)	634 (247)	357 (140)	470 (179)	292 (87)	389 (186)
DIN	70 (43)	139 (115)	72 (42)	104 (74)	54 (28)	86 (57)
Si	1.57 (0.79)	2.59 (1.36)	1.03 (0.70)	1.54 (0.95)	1.19 (0.51)	1.76 (0.64)
CHL	5.6 (2.1)	8.0 (3.8)	4.5 (1.9)	6.4 (2.4)	2.9 (1.4)	5.6 (3.2)
CDOM	29 (27)	47 (56)	14 (12)	15 (13)	15 (11)	18 (22)
SD	1.2 (0.4)	1.0 (0.3)	1.3 (0.5)	1.0 (0.4)	1.4 (0.4)	1.0 (0.3)

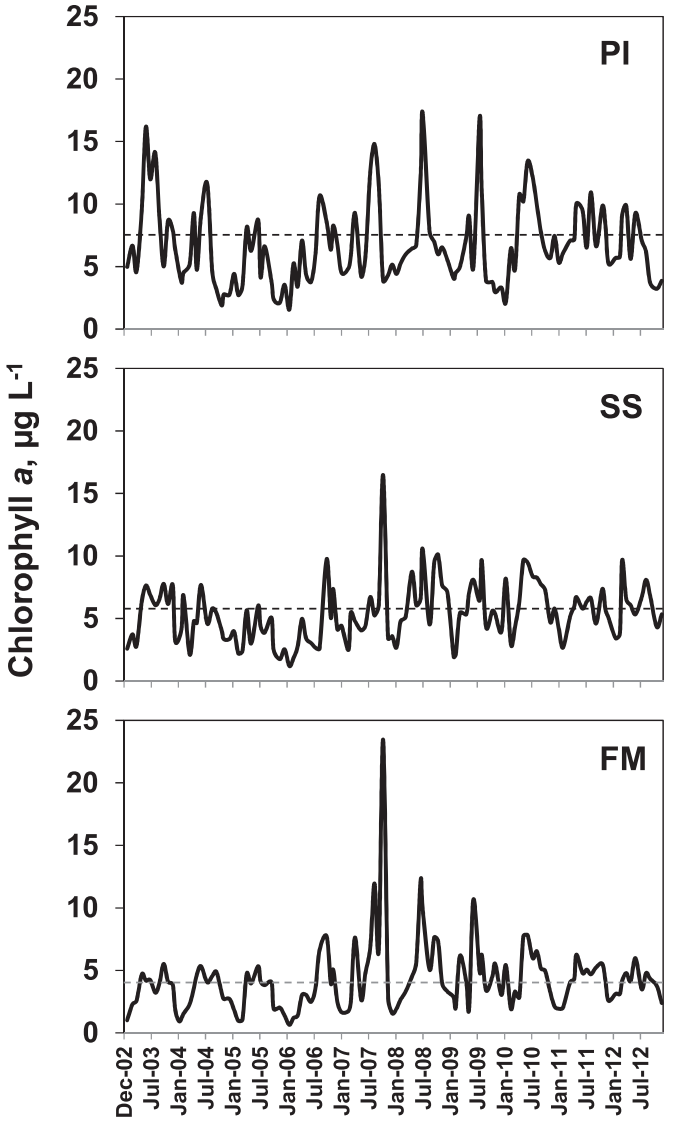

Fig. 5. Chlorophyll *a* at the three sampling sites; PI (top panel), SS (middle panel) and FM (bottom panel). Dotted line represents mean concentration over the study period, i.e. 6.8, 5.4 and 4.3 µg L^{-1} at PI, SS and FM, respectively.

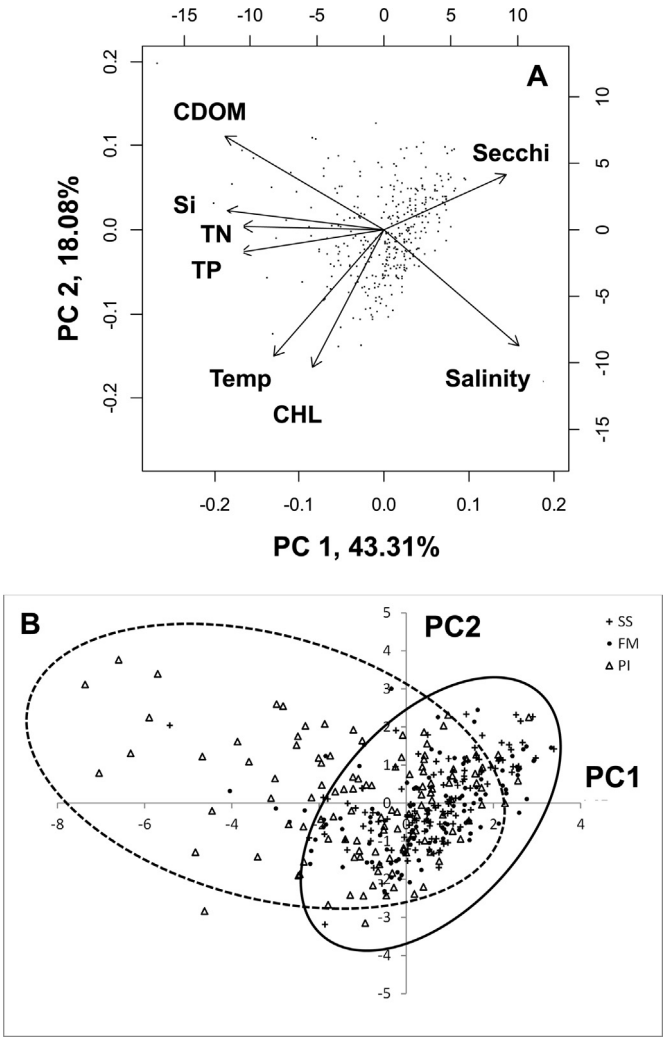

Fig. 6. PCA results on PC1 and PC2 space highlight (A) the biplot showing relationships among environmental factor loadings, and (B) the distributions of regional samples among different sampling sites. SS samples designated as plus signs, FM as filled circles and PI as open triangles. Dashed line oval encloses most samples from PI, while solid line oval encloses most samples from SS and FM.

From a regional perspective, the distribution of data points for SS and FM in the PCA are closely related, as illustrate by the black distribution oval in Fig. 6B. By contrast, the distribution of data points for PI (i.e. dashed line oval) did not completely overlap with points for SS and FM, revealing distinctions in the character of the Pine Island region from the St. Augustine and Matanzas regions.

In terms of the relationships between nutrient loads, nutrient concentrations and phytoplankton biomass, no significant positive regression relationships were observed between annual TP or TN loads and annual mean chlorophyll *a* concentrations at any of the sampling sites (Table 3). Similarly, no significant positive relationships were observed between mean wet season TP and TN concentrations and mean wet season chlorophyll *a* concentrations (Table 3). The lack of a positive relationship is further reflected in temporal trends for soluble reactive phosphorus (SRP) and dissolved inorganic nitrogen (DIN) in relationship to chlorophyll *a*. The lowest rainfall periods during the study, i.e.2006–2007 and 2010–2011, coincided with generally reduced levels of both SRP and DIN throughout the year, but relatively high peaks in chlorophyll *a* (Figs. 7 and 8).

The lack of strong positive relationships between nutrient loads and phytoplankton biomass is further indicated by the observation that the highest annual mean chlorophyll *a* concentrations (Fig. 9) were observed at PI despite being the region with the lowest TN and TP loads during all ten years of the study (Table 2).

The temporal relationships between peaks in rainfall and chlorophyll *a* indicate that major rainfall events or prolonged periods of high rainfall have negative effects on phytoplankton biomass. This pattern is illustrated by the data from PI, which shows that peaks in chlorophyll *a* preceded major rainfall events or occurred during low rainfall periods (e.g. 2003, 2006, 2010 and 2011) (Fig. 10).

3.2. Phytoplankton biovolume and composition

Diatoms, dinoflagellates, and cyanobacteria were generally the dominant contributors to total phytoplankton biovolume over the study period at all three sampling sites (Fig. 11, Table 4). Other major groups included cryptophytes, euglenoids, and microflagellates (Fig. 11, Table 5). A number of species of freshwater chlorophytes (e.g. *Closterium* spp. *Scenedesmus* spp.) and cyanobacteria (e.g. *Anabaena circinalis*) were observed during high

Table 3
Relationships between mean chlorophyll *a* concentrations, nutrient loads (a and b) and mean nutrient concentrations (c and d) at the three sampling sites.

a. Annual total phosphorus load (x as kg ha^{-1}) versus annual mean chlorophyll *a* concentrations (y as μg L^{-1}).	
PI: y = −0.50x + 7.7	R^2 = 0.22
SS: y = −0.09x + 6.5	R^2 = 0.24
FM: y = 0.02x + 4.1	R^2 = 0.01
b. Annual total nitrogen load (x as kg ha^{-1}) versus mean wet season chlorophyll *a* concentrations (y as μg L^{-1}).	
PI: y = −0.04x + 7.7	R^2 = 0.22
SS: y = −0.01x + 6.5	R^2 = 0.22
FM: y = 0.002x + 4.2	R^2 = 0.01
c. Mean wet season total phosphorus concentrations (x as mg L^{-1}) versus mean wet season chlorophyll *a* concentrations (y as μg L^{-1}).	
PI: y = 40.5x + 4.9	R^2 = 0.07
SS: y = 0.8x + 6.3	R^2 < 0.001
FM: y = −93.4x + 10.8	R^2 = 0.14
d. Mean wet season total nitrogen concentrations (x as mg L^{-1}) versus mean wet season chlorophyll *a* concentrations (y as μg L^{-1}).	
PI: y = −1.4x + 8.9	R^2 = 0.01
SS: y = 0.05x + 6.3	R^2 < 0.001
FM: y = 2.6x + 4.4	R^2 = 0.02

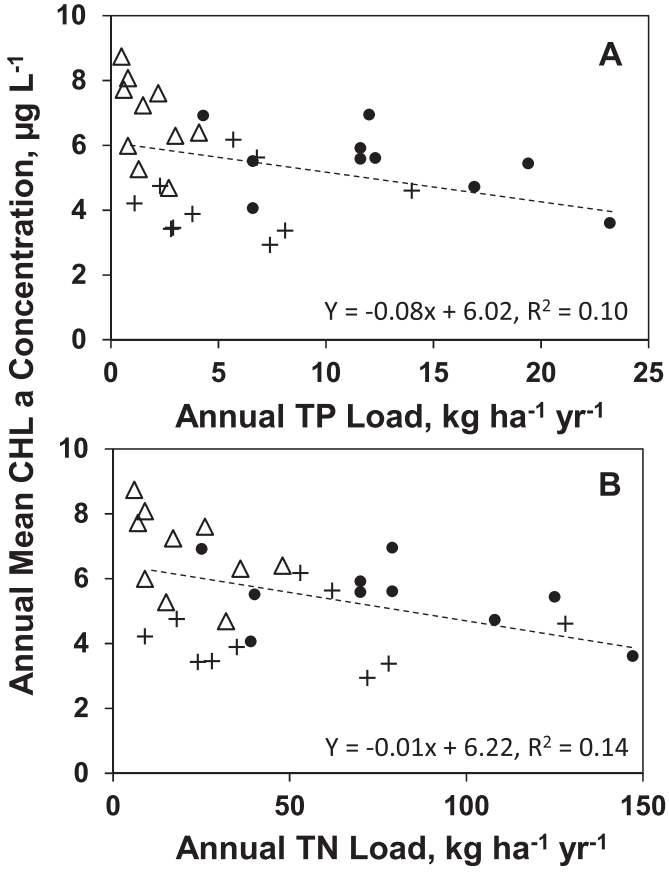

Fig. 7. Relationships between annual TP loads (A) and annual TN loads (B) in the three segments of the GTM (i.e. Pine Island, San Sebastian and Fort Matanzas), and annual mean chlorophyll *a* concentrations at associated sites PI (open triangle), SS (solid circle) and FM (plus sign). The linear regression relationship for all sites combined is shown as a dashed line, with equation and R^2 shown below.

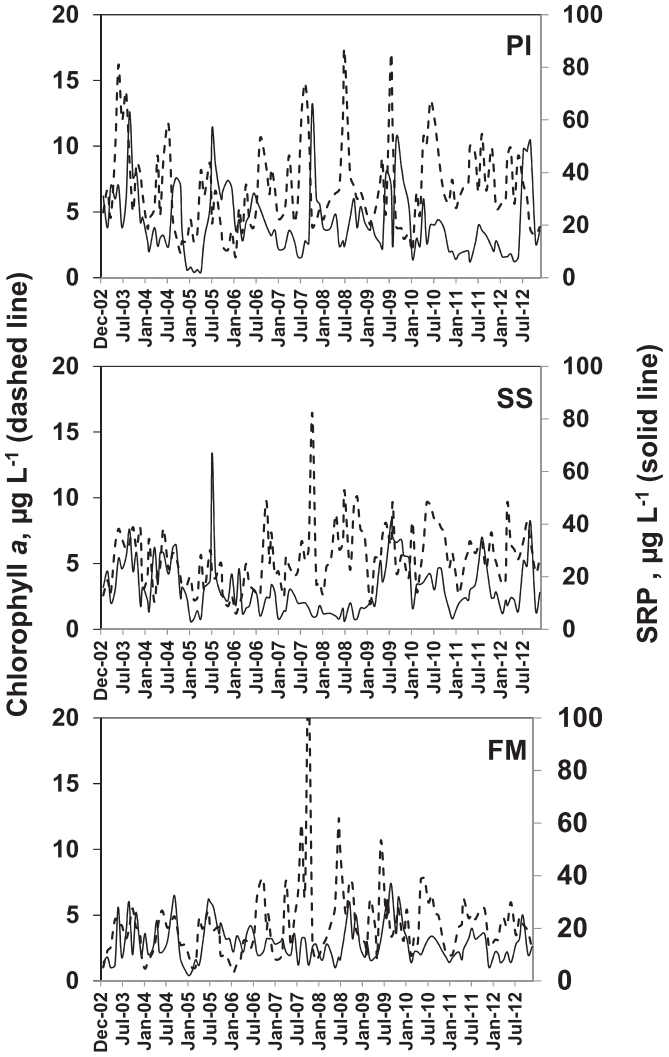

Fig. 8. Chlorophyll *a* and soluble reactive phosphorus (SRP) concentrations at the three sampling sites; PI (top panel), SS (middle panel) and FM (bottom panel).

rainfall periods, likely due to watershed inputs, but did not reach significant biovolume levels (Table 5).

Diatoms were on average the most often dominant group in terms of biovolume at all three sites (Table 4). Both centric and pennate diatoms were abundant throughout the GTM, among them *Cerataulina pelagica, Chaetoceros* spp., *Guinardia* spp., *Leptocylindrus* spp., *Navicula* spp., *Nitzschia* spp., *Odontella* spp., *Paralia sulcata, Pleurosigma-Gyrosigma* spp., *Rhizosoloenia setigera, Skeletonema costatum,* and *Thalassionema nitzschioides* (Table 5). The potentially toxic pennate diatoms *Pseudo-nitzschia calliantha* and *Pseudo-nitzschia turdigula* were also observed, but at relatively low biovolumes (Table 5).

Dinoflagellates were on average more prominent at Sites SS and FM than Site PI (Table 4). The most important dinoflagellate groups in terms of biovolume included *Ceratium* spp., *Gonyaulax polygramma*, Gymnoid spp., *Gyrodinium* spp., *Prorocentrum* spp., and *Protoperidinium* spp. (Table 5). A large bloom of the toxic marine dinoflagellate *Karenia brevis* was observed at Sites FM and SS in October 2007 (Fig. 9), a result of an incursion of coastal water containing a bloom of the species. Additionally, potentially toxic or other problematic harmful algae bloom (i.e. HAB) species observed during the study period included Akashiwo sanguinea, Cochlodinium polykrikoides, Dinophysis caudata, *Gyrodinium instriatum, Karlodinium veneficum, Kryptoperidinium foliaceum, Oxyphysis oxytoxoides, Peridinium quinquecorne, Prorocentrum mexicanum* (aka *P. rathymum), Prorocentrum minimum* and *Takayama tasmanica*

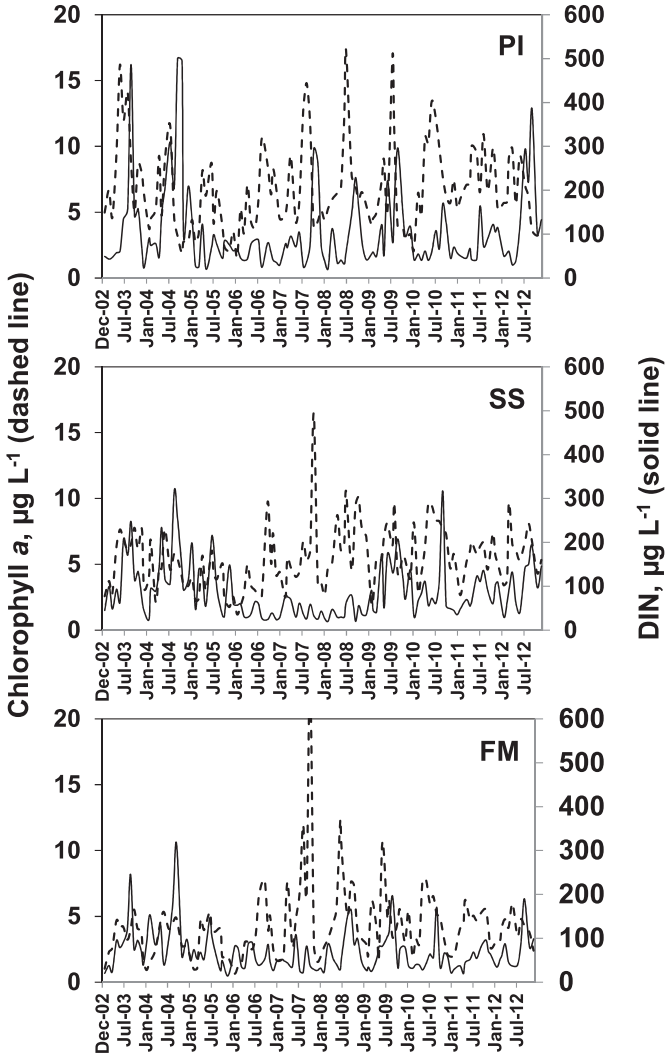

Fig. 9. Chlorophyll *a* and dissolved inorganic nitrogen (DIN) concentrations at the three sampling sites; PI (top panel), SS (middle panel) and FM (bottom panel).

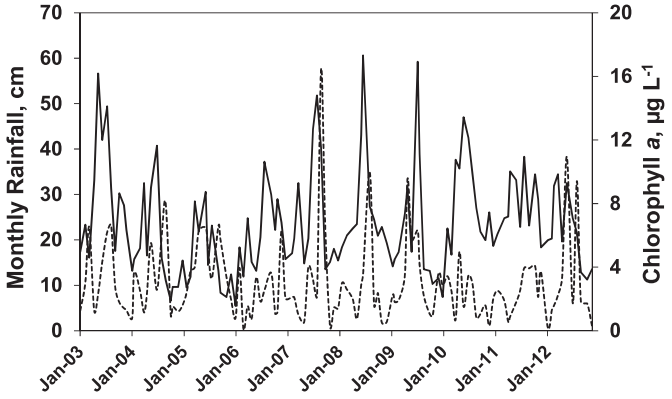

Fig. 10. Chlorophyll *a* concentrations (solid line) at PI and monthly rainfall totals (dashed line) from 2003 to 2012.

(Table 5). However, biovolumes of these species were not observed at bloom levels.

Picophytoplankton contributed significantly to the phytoplankton community at all three sites in the GTM, and were most

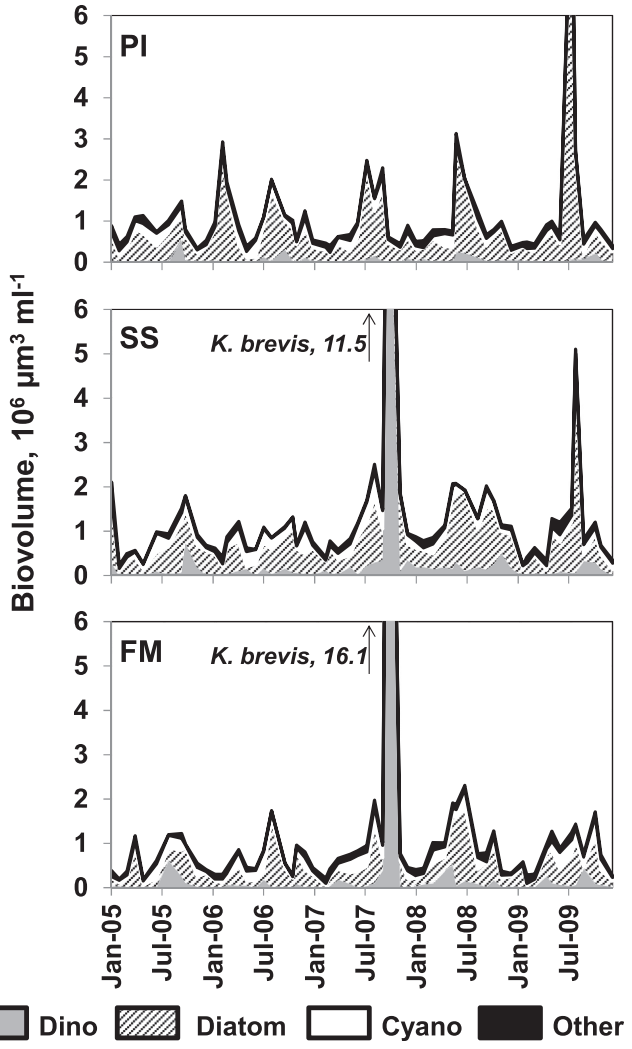

Fig. 11. Phytoplankton biovolume by major group at the three sampling sites; PI (top panel), SS (middle panel) and FM (bottom panel). Dinoflagellates in grey, diatoms in cross hatch, cyanobacteria in white and all other taxa in black.

Table 4
Mean percent of total biovolume represented by four major groupings of phytoplankton: i.e. dinoflagellates (Dino), diatoms (Diatom), cyanobacteria (Cyano), and all other algae (Other).

Site	Dino	Diatom	Cyano	Other
PI	6%	64%	17%	13%
SS	14%	57%	19%	10%
FM	12%	50%	23%	15%

often numerically dominant, but only occasionally dominant in terms of total phytoplankton biovolume (Table 4).

The average size distribution of phytoplankton taxa varied between sampling sites (Table 6). Picoplanktonic and nanoplanktonic species (i.e. 0.5–20 µm) were on average a higher percent of total biovolume at sites SS and FM than PI. Conversely, microphytoplankton (i.e. >20 µm) were on average a higher percent of total biovolume at site PI than SS or FM. This trend is further illustrated by the observation that the phytoplankton group with the highest mean biovolume from 2005 to 2009 was large-celled (i.e. 30–100 µm) diatoms at PI, but picoplanktonic spherical cyanobacteria at SS and FM (Table 7).

Table 5
Phytoplankton taxa observed from 2005 to 2009 at the three sampling sites. Asterick (*) indicates a potentially harmful algae bloom species i.e. (HAB species).

Group	Highest biovolume μm^3 ml^{-1}	# Obs.	Group continued	Highest biovolume μm^3 ml^{-1}	# Obs.
Chlorophytes					
Ankistrodesmus convolutus	367	1	*Chaetoceros danicus*	344,200	3
Chlorogonium sp.	2044	2	*Chaetoceras* spp.	454,081	21
Closterium spp.	13,315	10	Centric diatom spp. ≤30 μ	473,660	177
Crucigenia spp.	4132	3	Centric diatom spp. >30–100 μ	3,216,018	170
Kirchneriella sp.	148	1	Centric diatom spp. >100 μ	5,015,524	23
Pediastrum simplex	94	1	*Cerataulina pelagica*	249,922	15
Scenedesmus bijuga	297	4	*Dactyliosolen fragilissimus*	314,593	47
Scenedesmus intermedius	339	1	*Guinardia* spp.	275,542	8
Tetrastrum sp.	4316	1	*Guinardia striata*	18,812	15
			Hemialus hauckii	51,649	6
Euglena			*Hemialus sinensis*	28,260	12
Euglena spp.	271,169	18	*Leptocylindrus danicus*	348,856	3
			Leptocylindrus minimus	70,329	11
Dinoflagellates			*Licmophora* sp.	1060	2
*Akashiwo sanguinea**	20,561	8	*Melosira* spp.	4000	3
Ceratium fusus	8394	6	*Navicula* spp. ≤25 μ	12,551	16
Ceratium hircus	72,904	12	*Navicula* spp. >25 μ	512,092	35
Ceratium lineatum	206,543	31	*Nitzchia* sp.	18,197	127
*Cochlodinium polykrikoides**	55,619	7	*Nitzschia* spp. 50–100 μ	37,241	33
*Dinophysis caudata f. acutiformis**	12,095	16	*Nitzschia* spp.100–200 μ	24,484	92
Gonyaulax polygramma	191,389	19	*Odontella aurita*	569,671	14
Gonyaulax scrippsae	718	2	*Odontella mobilienis*	294,303	68
Gymnoid spp.≤15 μ	68,164	127	*Odontella regia*	1,897,658	36
Gymnoid spp. >15 μ	111,425	52	*Paralia sulcata*	616,222	98
*Gyrodinium instriatum**	85,367	31	Pennate diatom spp. ≤15 μ wide, 5–75 μ long	357,249	177
Gyrodinium pinque	136,308	29	Pennate diatom spp. ≤15 μ wide, 76–250 μ long	95,480	71
Gyrodinium spirale ≤80 μ	211,425	83	Pennate diatom spp. ≤15 μ wide, >250 μ long	1,036,460	28
Gyrodinium spirale >80 μ	130,314	16	Pennate diatom spp. >15 μ wide, 25–100 μ long	154,943	97
Hermesinum adriaticum	1275	3	Pennate diatom spp. >15 μ wide, >100 μ long	319,725	50
*Karenia brevis**	15,304,271	2	*Pleurosigma/Gyrosigma* spp. ≤20 μ	100,801	143
*Karlodinium veneficum**	56,820	2	*Pleurosigma/Gyrosigma* spp. >20 μ	229,109	106
Katodinium glaucum	854	2	*Pseudo-nitzschia calliantha**	12,726	12
*Kryptoperidinium foliaceum**	152,591	2	*Pseudo nitzchia turgidula*	18,735	8
*Oxyphysis oxytoxoides**	26,933	32	*Rhizosolenia setigera*	694,236	78
*Peridinium quinquecorne**	150,550	2	*Skeletonema costatum*	1,028,528	56
Podolampas palmipes	30,476	17	*Striatella unipunctata*	6250	3
Protoperidinium bipes	118,412	1	*Surirella* sp.	4793	1
Prorocentrum gracile	59,593	31	*Thalassionema nitzschioides*	281,281	79
*Prorocentrum mexicanum**	102,509	68			
Prorocentrum micans	260,201	49	**Cyanobacteria**		
*Prorocentrum minimum**	347,198	2	*Anabaena* spp.*	24,841	3
Protoperidinium pellucidium	3589	1	*Anabaena circinalis**	80,684	3
Protoperidinium spp.≤30 μ	754,945	9	*Oscillitoria* spp.	50,476	21
Protoperidinium spp. >30 μ	126,718	61	*Pseudoanabaena* spp.	3956	3
Pyrophacus spp.	82,046	19	Spherical picoplanktonic cyanobacteria	617,047	177
Scrippsiella subsalsa	5585	1	*Synechococcus* spp.	243,697	81
*Takayama tasmanica**	59,122	2			
			Other Microflagellates		
Cryptophytes			*Chattonella* sp.*	1586	1
Cryptophyte spp. ≤15 μ	190,208	177	Ovoid flagellate spp. ≤15 μ	18,653	103
Cryptophyte spp. >15 μ	38,691	31	Ovoid flagellate spp. >15 μ	41,039	8
			Prymnesium sp.*	11,198	3
Diatoms			Spherical flagellate sp.4–6 μ	81,479	164
Asterionella glacialis	19,008	4	Spherical flagellate sp. 8-10μ	3164	4
Bellerocha sp.	162,881	9	Spherical flagellate spp. ≤10 μ	11,148	166
Biddulphia spp.	113,044	24	Spherical flagellate spp. >10 μ	115,863	31

Table 6
Mean percent of total phytoplankton biovolume represented by three size classes: i.e. picophytoplankton (Pico, ≈ 0.5–3 μm), nanophytoplankton (Nano, >3 and ≤20 μm), and microphytoplankton (Micro, >20 μm).

Site	Pico	Nano	Micro
PI	12%	36%	52%
SS	13%	53%	34%
FM	16%	61%	23%

4. Discussion

The primary objective of this study was to compare trends in phytoplankton biomass and species composition in three regions of the GTM subject to differing nutrient loads and water residence times. Results of the study reveal that regional differences in hydrodynamic conditions, as well as temporal shifts in climatic conditions (i.e. principally rainfall levels), help to explain observed spatial and temporal differences in phytoplankton biomass and composition. The impacts of hydrology and climate can be viewed from two perspectives: the role of water residence time and the effects of allochthonous inputs.

4.1. Influence of water residence time and climate on phytoplankton biomass

The dampening effects of high rates of tidal water exchange or

Table 7
Top five phytoplankton groups observed in nearly all samples (i.e. out of 59 samples), in terms of mean biovolume (as 10^3 μm^3 ml^{-1}).

Site	Phytoplankton	Mean	Number of observations
	Group	Biovolume	
PI	Centric diatoms (30–100 μm)	281	59
	Spherical picocyanobacteria (0.7–2 μm)	135	59
	Cryptophytes (5–20 μm)	86	59
	Centric diatoms (<30 μm)	71	59
	Pennate diatoms (<30 μm)	52	59
SS	Spherical picocyanobacteria (0.7–2 μm)	172	59
	Centric diatoms (30–100 μm)	152	58
	Centric diatoms (<30 μm)	69	58
	Cryptophytes (5–20 μm)	63	59
	Pennate diatoms (<30 μm)	61	59
FM	Spherical picocyanobacteria (0.7–2 μm)	164	59
	Centric diatoms (30–100 μm)	82	54
	Cryptophytes (5–20 μm)	77	59
	Pennate diatoms (<30 μm)	53	59
	Centric diatoms (<30 μm)	52	59

freshwater discharge on phytoplankton biomass in estuaries have been previously documented in a number of systems, such as the Neuse River Estuary in North Carolina (Paerl et al., 2014) and Pearl River Estuary in China (Harrison et al., 2008; Lu and Gan, 2014). These observations highlight the difficulty of modeling the relationships between nutrient levels and biomass in physically dynamic coastal ecosystems (Cloern, 2001; Lucas et al., 2009). The lack of significant positive relationships between nutrient loads, nutrient concentrations, and phytoplankton biomass (i.e. in terms of chlorophyll *a*) in the GTM highlight the importance of such mitigating factors, particularly as it relates to water residence times and freshwater flushing (Dix et al., 2013). The effect of short water residence times on phytoplankton biomass are illustrated by the observation that the most tidally flushed regions of the GTM near the St. Augustine and Matanzas Inlets are associated with lower average phytoplankton biomass than suggested by nutrient loads and concentrations (Dix et al., 2013). The impact of high rates of tidal water exchange with the Atlantic Ocean at SS and FM is also demonstrated by the higher nutrient levels at PI, despite lower nutrient loads than in the former two regions.

The importance of water residence time in the regulation of phytoplankton biomass is further indicated by the comparatively high peaks in phytoplankton biomass and annual mean chlorophyll *a* concentrations at PI in the northern GTM, where nutrient loads are lower than in either the San Sebastian or Fort Matanzas regions, but water residence times are longer, because of the greater distance of PI from the St. Augustine Inlet and the presence of a tidal node just north of PI. For example, a recent estimate of water residence times (i.e. E_{50}, 50% water replacement interval) for April–May 2004 revealed mean values of 2 days in the Fort Matanzas region, 3 days in the San Sebastian region, but 15 days in the Pine Island region (Sheng et al., 2008). During the same period peak chlorophyll *a* levels reached 12 μg L^{-1} at PI, but only 7 μg L^{-1} at SS and 5 μg L^{-1} at FM, perhaps in part due to differences in water residence times. Similarly, in 2004 the annual mean chlorophyll *a* concentrations at PI (i.e. 5.4 μg L^{-1}) was higher than at SS (i.e. 4.6 μg L^{-1}) or FM (i.e. 3.4 μg L^{-1}), but annual TN and TP loads were considerably lower in the region of PI (i.e. 15 kg ha^{-1} TN and 1.3 kg ha^{-1}) than SS (i.e. 108 kg ha^{-1} TN and 17 kg ha^{-1}) or FM (i.e. 78 kg ha^{-1} TN and 8.1 kg ha^{-1}).

Another indication of the importance of rainfall-related changes in regional flushing rates is the negative relationship of high rainfall periods to phytoplankton biomass in the GTM, as illustrated by the observation that peaks in chlorophyll *a* generally preceded major peaks in rainfall or occurred during periods of low rainfall, most likely due to increased flushing rates, and in the case of PI, declines in salinity. Similar observations have been made in other coastal ecosystems around the world where differences in flushing rates and water residence times play a major role in defining biomass potential (Knoppers et al., 1991; Alpine and Cloern, 1992; Delesalle and Sournia, 1992; Monbet, 1992; Trigueos and Orive, 2000; Abreu et al., 2010; Cloern and Jassby, 2010; Zingone et al., 2010; Odebrecht et al., 2015), including other estuaries in Florida, such as the Indian River Lagoon (Phlips et al., 2004, 2011), Florida Bay (Phlips et al., 1999), Tampa Bay (Badylak et al., 2007), and the Caloosahatchee estuary (Badylak et al., 2014).

Despite the short water residence times in regions of the GTM near inlets, there is evidence that there are increases in phytoplankton biomass over the concentrations in the adjacent coastal environment. Average chlorophyll *a* concentrations in the GTM over the study period (i.e. 4.3 μg L^{-1} at FM, 5.4 μg L^{-1} at SS and 6.8 μg L^{-1} at PI) were twice as high as average chlorophyll *a* levels observed using satellite imagery of near shore coastal areas near the St. Augustine and Matanzas Inlets over the same time period (i.e. 2.8 μg L^{-1} outside of St. Augustine Inlet and 2.1 μg L^{-1} outside of Matanzas Inlet) (Blake Schaeffer, USEPA, personal communication), indicating an increase in phytoplankton biomass within the estuary. The difference also suggests that, on average, phytoplankton growth rates exceed loss processes in the GTM, including grazing (Dix et al., 2013). However, the short water residence times associated with the St. Augustine and Matanzas regions appear to preclude the full expression of biomass potential represented by bioavailable nutrient levels (Dix et al., 2013), providing a level of resistance to eutrophication. Similar observations have been made in other well-flushed freshwater and marine ecosystems (Howarth et al., 2000; Caraco et al., 2006; Lucas et al., 2009).

4.2. Influence of water residence time on phytoplankton composition

Differences in water residence times between regions in the GTM are also reflected in the structure of the phytoplankton communities. Phytoplankton communities in all three regions of the GTM are generally dominated by diatoms (i.e. 50–64% of mean total biovolume), along with significant contributions by picoplanktonic cyanobacteria, dinoflagellates and cryptophytes. All three regions of the GTM examined in this study have relatively short water residence times (i.e. days-weeks) compared to ecosystems with very slow water turnover rates, such as the northern Indian River Lagoon in Florida, where water residence times range

from months, up to a year (Phlips et al., 2004, 2010, 2015). These differences are reflected in the prominence of large slow-growing dinoflagellates in the latter ecosystem, while faster-growing diatoms, phyto-flagellates and picoplanktonic cyanobacteria are major players in the GTM. Short water residence times favor faster growing phytoplankton groups (Smayda and Reynolds, 2001; Murrell and Lores, 2004; Reynolds, 2006; Quinlan and Phlips, 2007).

There are noteworthy differences in the specific character of phytoplankton communities at the three sampling sites in the GTM, which may reflect differences in water residence times between PI, where water residence time can exceed 10 days, and the more rapidly flushed regions of the GTM (i.e. FM and SS), where water residence times are generally less than 5 days (Sheng et al., 2008). In terms of mean relative contribution to total phytoplankton biovolume, pico- and nanoplanktonic (0.5–20 μm) species together represented 66 and 77% of totals at FM and SS, respectively, but only 48% at PI. Conversely, microphytoplankton (i.e. 20–200 μm) represented a mean 52% of total biovolume at PI, compared to 34 and 23% at FM and SS respectively. The elevated relative importance of larger-celled phytoplankton at PI relative to FM and SS is further reflected in the observation that larger centric diatoms (i.e. 30–100 μm) were the single most prominent phytoplankton group on a biovolume basis at PI, while picocyanobacteria were the largest single contributors at FM and SS.

In more general terms, the character of the phytoplankton communities in the GTM fit well into the concepts of competition between r-versus K-selected species (Kilham and Kilham, 1980), and the more recent extension of these concepts in the C–S–R model of phytoplankton succession (Smayda and Reynolds, 2001; Reynolds, 2006). The high level of representation of small fast-growing species in the GTM reflects the advantages 'r-selected' species (i.e. 'C'-selected species in the C–S–R model) have in environments with high water turnover rates, but low probability of extended periods of nutrient limitation, both of which describe the general conditions in the GTM. Beyond this general pattern, the greater presence of larger microphytoplankton species (e.g. 30–100 μm centric diatoms) at PI may reflect the incrementally longer water residence times than at SS and FM. The larger presence of microphytoplankton at PI than at SS and FM may also reflect spatial differences in top-down pressure within the GTM. Specifically, oyster populations in the regions of sites SS and FM are considerably larger than in the Pine Island region (Dix et al., 2013), which may play a role in structuring the phytoplankton population through selective grazing of microphytoplankton (Alpine and Cloern, 1992; Cloern and Dufford, 2005; Sunda and Shertzer, 2012).

4.3. Allochthonous influences on phytoplankton biomass and composition

Phytoplankton biomass in the GTM was also influenced by exchange of water with the Atlantic Ocean. Tidally-flushed ecosystems, like the GTM, are subject to allochthonous influences from local watersheds and adjacent coastal waters. This is reflected in the frequent observation of cosmopolitan coastal phytoplankton species in the GTM, such as the diatom species *C. pelagica, Odontella regia, R. setigera* and *S. costatum* (Reynolds, 2006), and small picoplanktonic cyanobacteria (Flombaum et al., 2013).

Well-flushed estuaries can also be subject to periodic incursions of marine harmful algal blooms (HABs) (Steidinger, 1983; Tester et al., 1991; Hallegraeff, 2003; Heil et al., 2014). During the study period, bloom concentrations of the toxic red tide species *K. brevis* were observed in October 2007 at SS and FM. Similar incursions of *K. brevis* have been frequently observed in estuaries along the west coast of Florida, but are much less common on the east coast (Heil et al., 2014). *K. brevis* is known to be sensitive to salinities below 25 psu, but the high salinities experienced at SS and FM due to strong tidally-driven water exchange, likely facilitated the persistence of high *K. brevis* cell densities. *K. brevis* was not observed at PI, either due to less tidal influence or lower salinities at the site.

The intensity of the *K. brevis* incursion into the GTM resulted in fish kills and concerns about human health (http://www.staugustine.com/stories/101907/news_news_046.shtml), including widespread reports of symptoms associated with exposure to aerosolized algal neurotoxins (e.g. eye irritation and respiratory distress). The bloom event highlights the importance of allochthonous influences on phytoplankton dynamics and ecosystem health in well-flushed estuaries.

5. Summary

As part of the National Estuarine Research Reserve program of the U.S. National Oceanographic and Atmospheric Administration, one of the central goals of research in the GTM is to identify and address key management concerns for the ecosystem. One of these concerns is defining the potential for harmful algal bloom events which can impact the health of major components of the GTM, such as oyster communities that are important structural and functional components of the ecosystem (Frazel, 2009; Dix et al., 2013). As in many coastal environments around the world, the watersheds associated with the GTM are experiencing rapid human development, accompanied by the potential for future increases in nutrient loads and modifications in hydrology.

Defining the response of phytoplankton communities to changes in nutrient load is a major component of managing aquatic ecosystems, such as the establishment of Total Maximum Daily Load (i.e. TMDL) criteria (Steward and Lowe, 2010; Steward et al., 2010). The results of this study highlight the importance of hydrologic factors in defining the resilience of systems to eutrophication associated with increases in nutrient loads resulting from human activity. Overall, the well-flushed nature of much of the GTM provides the system with a degree of resilience to the type of intense algal blooms observed in more restricted ecosystems with significant nutrient inputs from anthropogenic sources (Hallegraeff, 2003; Glibert and Burkholder, 2006; Phlips et al., 2011, 2015). This general observation does not rule out the possibility of harmful algal blooms, particularly in parts of the GTM subject to longer water residence times, such as the Pine Island region. There is also a persistent risk of incursions of harmful algae blooms into the GTM from the Atlantic coast, as evidenced by the 2007 event involving the toxic red tide species *K. brevis*.

Acknowledgments

Research was conducted under a series of awards from the Estuarine Reserves Division, Office of Ocean and Coastal Resource Management, National Oceanic and Atmospheric Administration over the study period, i.e. 2002–2012.

References

Abreu, P.C., Bergesch, M., Procenca, L.A., Garcia, C.A., Odebrecht, C., 2010. Short- and long-term chlorophyll *a* variability in the shallow microtidal Patos Lagoon estuary, Southern Brazil. Estuaries Coasts 33, 54–569.

Adamus, C.L., Bergman, M.J., 1995. Estimating nonpoint source pollutant loads with a GIS screening model. Water Resour. Bull. 31, 647–655.

Alpine, A.E., Cloern, J.E., 1992. Trophic interactions and direct physical effects control phytoplankton biomass and production in an estuary. Limnol. Oceanogr. 37, 946–955.

Anderson, D.M., Burkholder, J.M., Cochlan, W.P., Glibert, P.M., Gobler, C.J., Heil, C.A., Kudela, R.M., Parsons, M.L., Rensel, J.E., Townsend, D.W., Trainer, V.L., Vargo, G.A., 2008. Harmful algal blooms and eutrophication: examining

linkages from selected coastal regions of the United States. Harmful Algae 8, 39–53.
APHA (American Public Health Association), 1998. Standard Methods for the Examination of Water and Wastewater, twentieth ed. United Book Press, Inc, Baltimore, Maryland, p. 1325.
Badylak, S., Phlips, E.J., Baker, P., Fajans, J., Boler, R., 2007. Distributions of phytoplankton in Tampa Bay, USA. Bull. Mar. Sci. 80, 295–317.
Badylak, S., Phlips, E.J., Mathews, A.L., 2014. *Akashiwo sanguinea* (Dinophyceae) blooms in a sub-tropical estuary: an alga for all seasons. Plankton Benthos Res. 9, 1–9.
Caraco, N.F., Cole, J.J., Strayer, D.L., 2006. Top-down control from the bottom: regulation of eutrophication in a large river by benthic grazing. Limnol. Oceanogr. 51, 664–670.
Carlson, R.E., 1977. A trophic state index for lakes. Limnol. Oceanogr 22, 361–369.
Cloern, J.E., 2001. Our evolving conceptual model of the coastal eutrophication problem. Mar. Ecol. Progr. Ser. 210, 223–253.
Cloern, J.E., Duffard, R., 2005. Phytoplnkton community ecology: principles applied in San Fransisco Bay. Mar. Ecol. Prog. Ser. 285, 11–28.
Cloern, J.E., Foster, S.Q., Kleckner, A.E., 2014. Phytoplankton primary production in the world's estuarine-coastal ecossytems. Biogeosceinces 11, 2477–2501.
Cloern, J.E., Jassby, A.D., 2010. Patterns and scales of phytoplankton variability in estuarine-coastal ecosystems. Estuaries Coasts 33, 230–241.
Delesalle, B., Sournia, A., 1992. Residence time of water and phytoplankton biomass in coral reef lagoons. Cont. Shelf Res. 12, 939–949.
Dix, N., Phlips, E.J., Gleeson, R., 2008. Water quality changes in a tidal creek within the Guana Tolomato Matanzas National Estuarine Research Reserve, Florida, associated with the four tropical storms of 2004. J. Coast. Res. Spec. Issue 55, 70–81.
Dix, N., Phlips, E.J., Suscy, P., 2013. Control of phytoplankton biomass in a well-flushed subtropical estuary in Florida, USA. Estuaries Coasts 36, 981–996.
FDEP (Florida Department of Environmental Protection), 2008. Upper East Coast Water Quality Assessment Report. Division of Environmental Assessment and Restoration, Tallahassee, Florida.
Frazel, D., 2009. Site Profile of the Guana, Tolomato, Matanzas National Estuarine Research Reserve. GTMNERR, Ponte Vedra, Florida, USA, p. 151.
Flombaum, P., Gallegos, J.L., Gordillo, R.A., Rincón, J., Zabala, L.L., Jiao, N., Karl, D.M., Li, W.K.W., Lomas, M.W., Veneziano, D., Vera, C.S., Vrugt, J.A., Martiny, A.C., 2013. Present and future global distributions of the marine cyanobacteria *Prochlorococcus* and *Synechococcus*. Proc. Nat. Acad. Sci. 10, 9824–9829.
Glibert, P.M., Burkholder, J.M., 2006. The complex relationships between increases in fertilization of the earth, coastal eutrophication and proliferation of harmful algae blooms. In: Granéli, E., Turner, J.T. (Eds.), Ecology of Harmful Algae. Springer-Verlag, Berlin, pp. 341–354.
Glibert, P.M., Dugdale, R.C., Wilkerson, F., Parker, A.E., Alexander, J., Antell, E., Blaser, S., Johnson, A., Lee, J., Murasko, S., Strong, S., 2014. Major – but rare – spring blooms in 2014 in San Francisco Bay Delta, California, a result of the long-term drought, increased residence time, and altered nutrient loads and forms. J. Exp. Mar. Biol. Ecol. 460, 8–18.
Green, W.C., 2013. Nutrient Loads in the GTM. Final Report, Contract CM107. Florida Department of Environmental Protection, Tallahassee, Florida.
Green, W.C., Steward, J.S., 2003. The utility of a pollutant load screening model in determining provision pollutant load reduction goals. In: Proceedings of the U.S. Environmental Protection Agency Technology Transfer Conference: Emerging Technologies, Tools and Techniques to Manage Our Coasts in the 21st Century. Cocoa Beach, Florida.
Gupta, M., 2014. A new trophic state index for lagoons. J. Ecosyst. http://dx.doi.org/10.1155/2014/152473.
Hallegraeff, G.M., 2003. Harmful algal blooms: a global overview. In: Hallegraeff, G.M., Anderson, D.M., Cembella, A.D. (Eds.), Manual on Harmful Marine Microalgae. Intergovernmental Oceanographic Commission of UNESCO, Paris, pp. 25–49.
Harding Jr., L.W., Adolf, J.E., Mallonee, M.E., Miller, W.D., Gallegos, C.L., Perry, E.S., Johnson, J.M., Sellner, K.G., Paerl, H.W., 2015. Climate effects on phytoplankton floral composition in Chesapeake Bay. Estuar. Coast. Shelf Sci. http://dx.doi.org/10.1016/j.ecss.2014.12.030.
Harrison, P.J., Yin, K.D., Lee, J.H.W., Gan, J.P., Liu, H.B., 2008. Physical-biological coupling in the Pearl River Estuary. Cont. Shelf Res. 28, 1405–1415.
Heil, C.A., Bronk, D.A., Dixon, K.L., Hitchcock, G.L., Kirkpatrick, G.J., Mullholland, M.R., O'Neil, J.M., Walsh, J.J., Weisberg, R., Garrett, M., 2014. The Gulf of Mexico ECOHAB: *Karenia* program 2006–2012. Harmful Algae 38, 3–7.
Heisler, J.P., Gilbert, P.M., Burkholder, J.A., Anderson, D.M., Cochlan, W., Dennison, W., Dortch, Q., Gobler, C.J., Heil, C., Humphries, E., Lewitus, A., Magnien, R., Marshall, H., Sellner, S., Stockwell, D., Stoecker, D., Suddleson, M., 2008. Eutrophication and harmful algal blooms: a scientific consensus. Harmful Algae 8, 3–13.
Howarth, R.W., Swaney, D.P., Butler, T.J., Marino, R., 2000. Climatic control of eutrophication of the Hudson River Estuary. Ecosystems 3, 210–215.
Kilham, P., Kilham, S.S., 1980. The evolutionary ecology of phytoplankton. In: Morris, I. (Ed.), The Physiological Ecology of Phytoplankton. Blackwell Publ., Oxford, pp. 571–597.
Knoppers, B., Kjerfve, B., Carmouze, J.P., 1991. Trophic state and water turn-over time in six choked coastal lagoons in Brazil. Biogeochemistry 14, 147–166.
Lu, Z., Gan, J., 2014. Controls of seasonal variability of phytoplankton blooms in the Pearl River estuary. Deep-Sea Res. II. http://dx.doi.org/10.1016/j.dsr2.2013.12.011.
Lucas, L.V., Thompson, J.K., Brown, L.R., 2009. Why are diverse relationships observed between phytoplankton biomass and transport time? Limnol. Oceanogr. 54, 381–390.
Mallin, M.A., Cahoon, L.B., McIver, M.R., Parsons, D.C., Shank, G.C., 1999. Alternation of factors limiting phytoplankton production in the Cape Fear River Estuary. Estuaries 22, 825–836.
Monbet, Y., 1992. Control of phytoplankton biomass in estuaries: a comparative analysis of microtidal and macrotidal estuaries. Estuaries 15, 563–571.
Murrell, M.C., Lores, E.M., 2004. Phytoplankton and zooplankton dynamics in a subtropical estuary: importance of cyanobacteria. J. Plankton Res. 26, 371–382.
Nixon, S.W., 1995. Coastal marine eutrophication: a definition, social causes, and future concerns. Ophelia 41, 199–219.
Odebrecht, C., Abreu, P.C., Carstensen, J., 2015. Retention time generates short-term phytoplankton blooms in a shallow microtidal subtropical estuary. Estuar. Coast. Shelf Sci. 162, 35–44.
O'Neil, J.M., Davis, T.W., Burford, M.A., Gobler, C.J., 2012. The rise of harmful cyanobacteria blooms: the potential roles of eutrophication and climate change. Harmful Algae 14, 313–334.
Paerl, H.W., Hall, N.S., Peierls, B.L., Rossignol, K.L., Joyner, A.R., 2014. Hydrologic variability and its control of phytoplankton community structure and function in two shallow coastal lagoonal ecosystems: the Neuse and New River estuaries, North Carolina. USA. Estuaries Coasts 37 (Suppl. 1), S31–S45, 1. dx.doi.org/10.1007/s12237-013-9686-0.
Parsons, T.R., Maita, Y., Lalli, C.M., 1984. A Manual of Chemical and Biological Methods for Seawater Analysis. Pergamon Press, New York.
Phlips, E.J., Badylak, S., Lynch, T.L., 1999. Blooms of the picoplanktonic Cyanobacterium Synechococcus in Florida Bay. Limnol. Oceanogr. 44, 1166–1175.
Phlips, E.J., Love, N., Badylak, S., Hansen, P., John, C.V., Gleeson, R., 2004. A comparison of water quality and hydrodynamic characteristics of the Guana Tolomato Matanzas National Estuarine Research Reserve and the Indian River Lagoon in Florida. J. Coast. Res. 45, 93–109. Special Issue.
Phlips, E.J., Badylak, S., Christman, M., Lasi, M., 2010. Climate changes and temporal trends of phytoplankton composition, abundance and succession in the Indian River Lagoon, Florida, USA. Estuaries Coasts 33, 498–512.
Phlips, E.J., Badylak, S., Christman, M., Wolny, J., Garland, J., Hall, L., Hart, J., Landsberg, J., Lasi, M., Lockwood, J., Paperno, R., Scheidt, D., Staples, A., Steidinger, K., 2011. Scales of variability of harmful algae blooms in the Indian River, Florida, USA. Harmful Algae 10, 277–290.
Phlips, E.J., Badylak, S., Lasi, M., Chamberlain, R., Green, W., Hall, L., Hart, J., Lockwood, J., Miller, J., Steward, J., 2015. From red tides to green and brown tides: bloom dynamics in a restricted subtropical lagoon under shifting climatic conditions. Estuaries Coasts 38, 886–904. 10.1007/s12237-014-9874-6.
Quinlan, E.L., Phlips, E.J., 2007. Phytoplankton assemblages across the marine to low-salinity zone in a blackwater dominated estuary. J. Plankton Res. 29, 410–416.
Reynolds, C.S., 2006. Ecology of Phytoplankton. Cambridge University Press, Cambridge, UK, p. 535.
Sartory, D.P., Grobbelaar, J.U., 1984. Extraction of chlorophyll *a* from freshwater phytoplankton for spectrophotometric analysis. Hydrobiologia 114, 177–187.
Sheng, Y.P., Tutak, B., Davis, J.R., Paramygin, V., 2008. Circulation and flushing in the lagoonal system of the Guana Tolomato Matanzas National Estuarine Research Reserve (GTMNERR), Florida. J. Coast. Res. 55, 9–25. Special Issue.
Smayda, T.J., 1978. From phytoplankton to biomass. In: Sournia, A. (Ed.), Phytoplankton Manual. United Nations Educational. Scientific and Cultural Organization, Paris, pp. 273–279.
Smayda, T.J., 2008. Complexity in the eutrophication-harmful algal bloom relationship, with comment on the importance of grazing. Harmful Algae 8, 140–151.
Smayda, T.J., Reynolds, C.S., 2001. Community assembly in marine phytoplankton: application of recent models to harmful dinoflagellate blooms. J. Plankton Res. 23, 447–461.
Steidinger, K.A., 1983. A revaluation of toxic dinoflagellate biology and ecology. Progr. Phycol. Res. 2, 147–189.
Steward, J.S., Green, W.C., Miller, J.D., 2010. Using Multiple Lines of Evidence for Developing Numeric Nutrient Criteria for Tolomato-Matanzas estuary, Florida. St. Johns River Water Management District, Palatka, Florida.
Steward, J.S., Lowe, E.F., 2010. General empirical models for estimating nutrient load limits for Florida's estuaries and inland waters. Limnol. Ocean. 55, 433–455.
Sunda, W.G., Shertzer, K.W., 2012. Modeling ecosystem disruptive algal blooms: positive feedback mechanisms. Mar. Ecol. Progr. Ser. 447, 31–47.
Tester, P.A., Stumpf, R.P., Vukovich, F.M., Fowler, P.K., Turner, J.T., 1991. An expatriate red tide bloom: transportation, distribution and persistence. Limnol. Oceanogr. 36, 1053–1061.
Trigueros, J.M., Orive, E., 2000. Tidally driven distribution of phytoplankton blooms in a shallow macrotidal estuary. J. Plankton Res. 22, 969–986.
Utermöhl, H., 1958. Zur vervollkommnung der quantitativen phytoplankton-methodik. Mittl. Ver. fur Theoretische Angew. Limnol. 9, 1–38.
Vollenweider, R.A., 1976. Advances in defining critical loading levels for phosphorus in lake eutrophication. Mem. dell'Istituto Ital. Idrobiol. 33, 53–83.
Zingone, A., Phlips, E.J., Harrison, P., 2010. Multiscale variability of twenty-two coastal phytoplankton time series: a global comparison. Estuaries Coasts 33, 224–229.